Clinical research using ImageStream Cytometry

The ImageStream system combines high-speed image capture with image quantification to create a statistically powerful microscopy platform, enabling robust discrimination of cells based on their appearance. This document highlights clinically relevant applications of ImageStream as described in publications, posters and podium presentations. For more information, check out the website: (https://www.amnis.com)

Table of Contents:

Endosomal trafficking of SLE immune complexes in human monocytes

Summary: This ImageStream assay quantifies the C1q-induced subcellular trafficking of systemic lupus erythematosis (SLE) immune complexes (IC) within human monocytes. The ImageStream's high speed imaging capacity enabled analysis of 10,000 events per sample for robust statistics. The co-localization feature used (bright detail similarity) measures the pixel-by-pixel correlation between the SLE IC and CD71 (or LAMP-1) images.

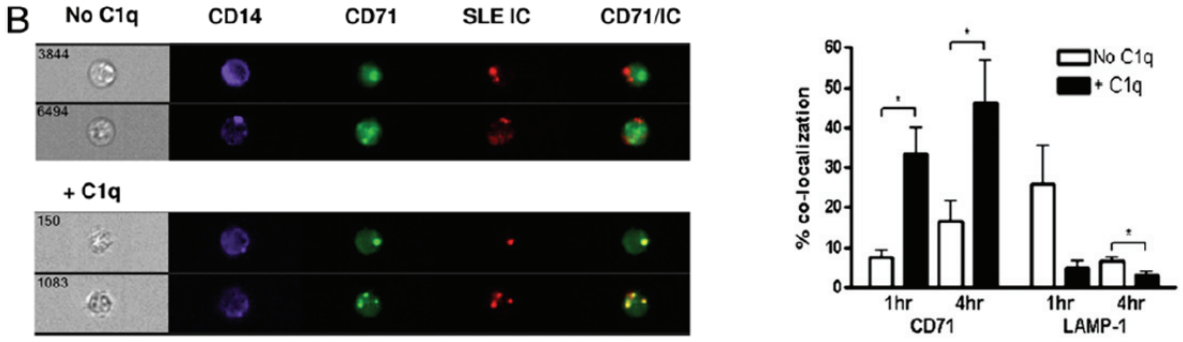

"Our study provides novel evidence to explain how C1q blocks IFN-α production. It demonstrates that C1q enhances the binding of ICs to both monocytes and pDCs. When monocytes were absent, C1q augmented IC binding to pDCs and led to increased IFN-α production. However, when monocytes were present, C1q preferentially and almost exclusively promoted the uptake of ICs by these cells, leading to accumulation in early endosomes and decreased IFN-α production by pDCs."

Reference: Santer, D.M., B.E. Hall, T.C. George, S. Tangsombatvisit, C.L. Liu, P.D. Arkwright, and K.B. Elkon, *C1q deficiency leads to the defective suppression of IFN-alpha in response to nucleoprotein containing immune complexes.* J Immunol, 2010. **185**(8): 4738-49.

~ ~ ~ ~ ~ ~

Preferential pDC-MDCC conjugate formation and transfer of cellular components with HSV infection

Summary: Analysis of the interaction of plasmacytoid dendritic cells (pDC) and monocyte-derived dendritic cells (MDDC) by imageStream cytometry combines the statistical robustness of the flow cytometer with the imaging sensitivity of microscopy. We observed that BDCA+ pDC (orange) preferentially formed conjugates (red gate) with the HSV-infected (B) vs. uninfected (A) CFSE+ MDDC (green) and preferentially took-up cellular components from the infected vs. the uninfected cells, as indicated by the increased percentage of single pDC (R3) with internalized CFSE.

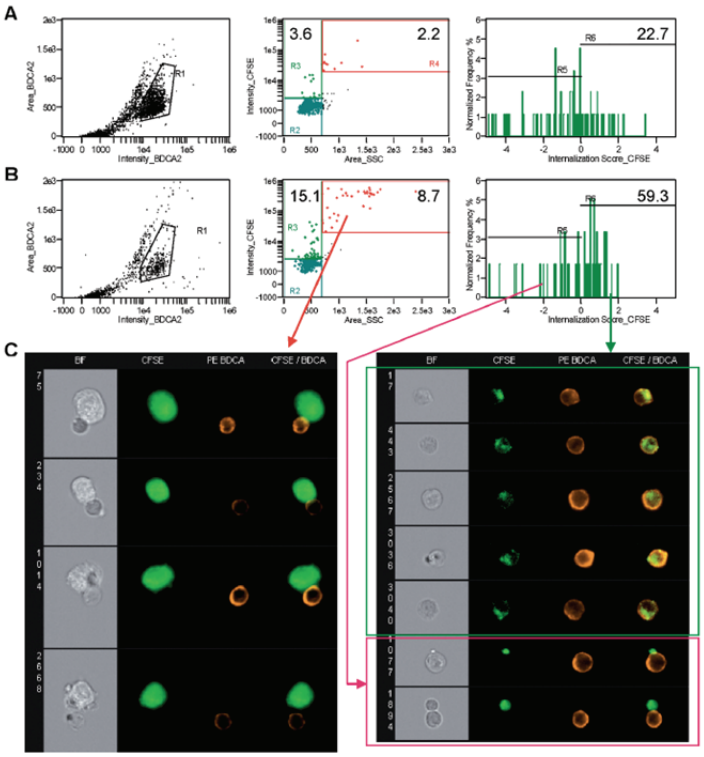

"In this study, we have evaluated the interaction of HSV-infected MDDC with pDC using a combination of traditional flow cytometric and imaging flow cytometric techniques. We report here that MDDC infected with HSV are able to stimulate IFN-α and chemokine production by pDC. Additionally, we demonstrate the preferential transfer of cellular components from HSVinfected MDDC vs. uninfected MDDC to pDC. Together, these results indicate that heterogeneous populations of DC interact to generate an effective IFN-α response."

Reference: Megjugorac, N.J., E.S. Jacobs, A.G. Izaguirre, T.C. George, G. Gupta, and P. Fitzgerald-Bocarsly, *Image-based study of interferongenic interactions between plasmacytoid dendritic cells and HSV-infected monocyte-derived dendritic cells.* Immunol Invest, 2007. **36**(5-6): 739-61.

Expression and maintenance of KHSV infection in tonsillar B cells

Summary: This ImageStream assay quantifies the expression and maintenance of Kaposi sarcoma–associated herpesvirus (KHSV) within human tonsillar B cells. KHSV-infected cells are identified as those events with latency-associated nuclear antigen (LANA) spots (A). Isolated B cells cultured in the presence of KHSV for 2-3 days (B) or for a 7day time course (C) demonstrate preferential growth of KHSV+ B cells. The ImageStream was further used to show that the cells expressing the λ-light chain of the B cell receptor were predominantly responsible for the observed maintenance of KHSV infection.

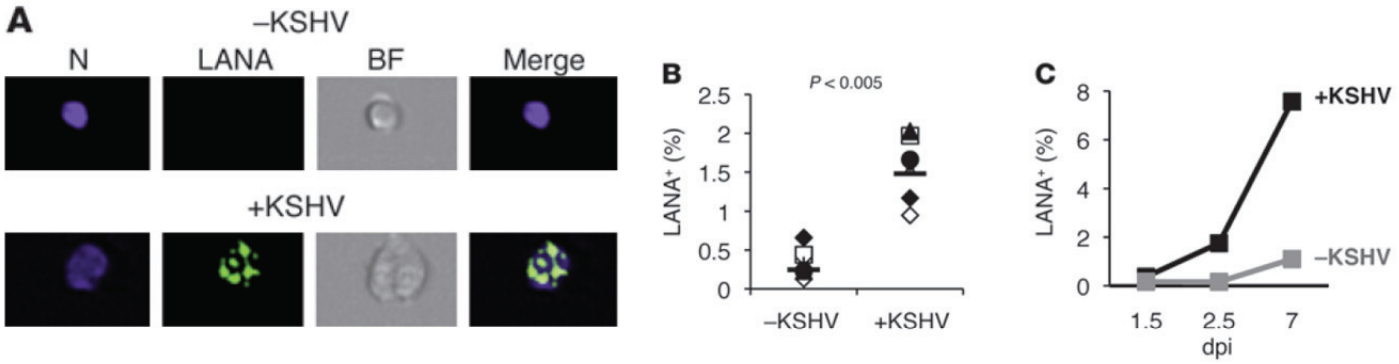

"To identify the cell type that potentially represents both the initial target of KSHV infection and the cell of origin for at least multicentric Castleman disease (MCD) and possibly primary effusion lymphoma (PEL), we exposed primary human tonsillar B cells to purified KSHV and characterized the cells that became latently infected using multispectral imaging flow cytometry (MIFC), a high-throughput single-cell imaging technique."

Reference: Hassman, L.M., T.J. Ellison, and D.H. Kedes, *KSHV infects a subset of human tonsillar B cells, driving proliferation and plasmablast differentiation.* J Clin Invest, 2010. **121**(2): 752-68.

~ ~ ~ ~ ~ ~

HIV-induced nuclear translocation of IRF3

Summary: This ImageStream assay measures IRF3 nuclear localization (by quantifying the similarity between the IRF3 and nuclear images on a per-cell basis) in 293T cells after co-culturing with MT4C5 cells. The ImageStream's unique ability to objectively measure translocation for thousands of cells per sample allows statistically robust discrimination of the samples, which is of critical importance given their heterogeneous response characteristics.

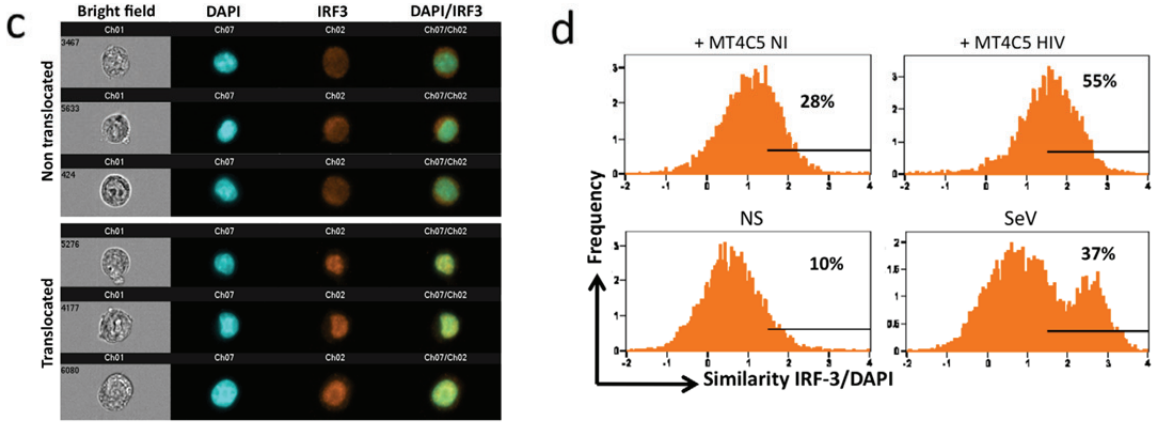

"A quantitative analysis based on the similarity of IRF3 and DAPI stainings revealed a 2-fold increase when 293T-4X4 were incubated with HIV-infected cells (55% vs 28% for cocultures of HIV-infected and non infected MT4C5 cells, respectively, Fig. 5d). As expected, with SeV, there was a 3-4-fold increase in the similarity score. Therefore, contact with HIV-infected cells induces nuclear translocation of IRF3 in 293T-4X4 cells."

Reference: Lepelley, A., S. Louis, M. Sourisseau, H.K. Law, J. Pothlichet, C. Schilte, L. Chaperot, J. Plumas, *et al.*, *Innate Sensing of HIV-Infected Cells.* PLoS Pathog, 2011. **7**(2): e1001284.

Measurement of TLR-mediated NF-κB nuclear translocation in whole blood pDC

Summary: This ImageStream assay measures NF-κB (pink) nuclear localization (by quantifying the similarity between the NF-κB and nuclear images on a per-cell basis) in CD123+BDCA-2+ pDC after incubation with the TLR-7 agonist R848. Median Similarity scores of pDC from whole blood samples incubated with the indicated dose of R848 for 60 minutes (bottom) or incubated for the indicated time with 1 μg/mL R848 (top) are plotted at right. Measuring nuclear translocation within non-enriched pDC, which account for ~0.1% of whole blood leukocytes, requires rapid imaging in order to obtain statistically relevant numbers of pDC for the translocation analysis.

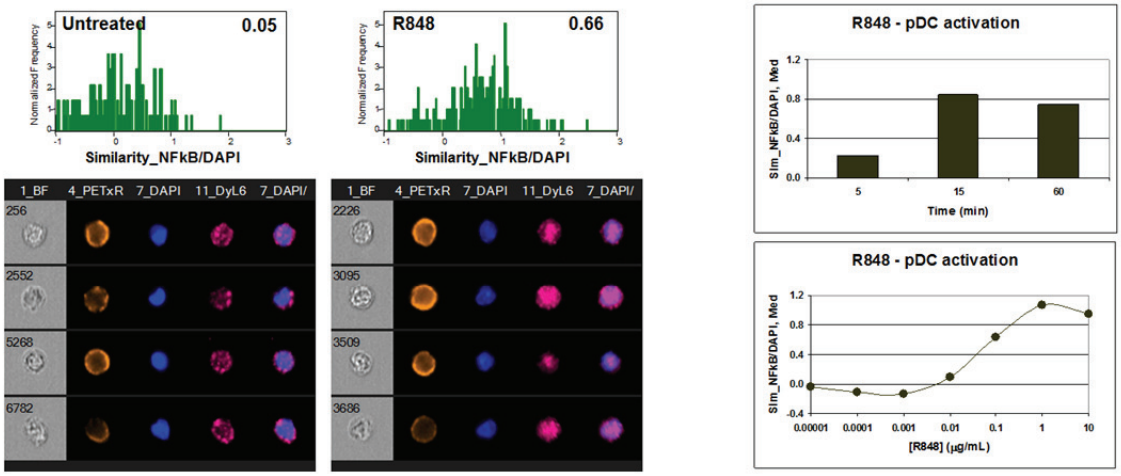

"Here we use imaging flow cytometry to quantify nuclear localization of NFkB in monocytes and pDC directly in whole blood samples. We show that very low doses (100 pg/mL) of LPS and TNF-a activate monocyte NFkB translocation within 5 minutes. We also show dose and time kinetics of TLR7 agonist R848-induced NFkB translocation of pDC directly in whole blood. These data demonstrate image-based measurement of nuclear translocation within rare cell and virus-specific innate immune cells using ImageStream technology."

Reference: T.C. George, B.E. Hall, S.M. Mordecai, S.L. Friend, and R. Kong, *Measurement of rare innate immune cell activation directly in whole blood using imaging flow cytometry.* Poster presentation AAI 2010.

~ ~ ~ ~ ~ ~

Inhibition of KHSV production with rapamycin treatment

Summary: This ImageStream assay quantifies intranuclear latency-associated nuclear antigen (LANA) spots as a measure of Kaposi sarcoma–associated herpesvirus (KHSV) titer obtained from infected BCBL-1 supernatants. Representative images of cells exposed to VPA-induced (left) or rapamycin-treated VPA-induced (right) BCBL-1 cells are shown in (A), with quantitative data for large event files of untreated (black) vs rapamycin-treated (grey) shown in (B). Rapamycin-mediated inhibition of cell-to-cell virus transmission (grey vs black) from spontaneously lytic BCBL-1 was assessed in (C).

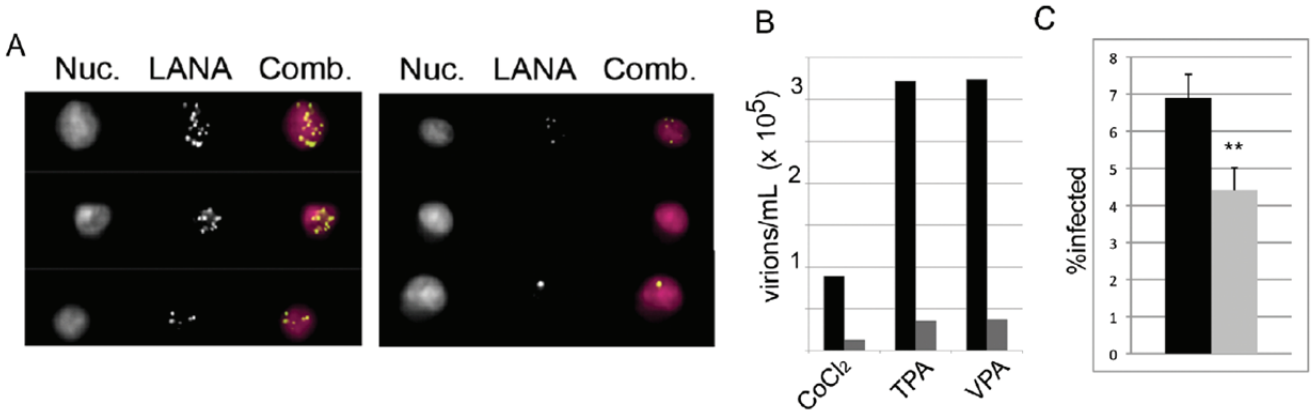

"While RTA is necessary and sufficient for initiating viral lytic replication, it is only the initial measure of the productive phase of infection. Clinically, the most important read-out is the production of virions… We measured titers of infectious virus by staining the KSHV-exposed HeLa cells for LANA and analyzing cells using multispectral imaging flow cytometry (MIFC) to determine the number of

punctate LANA dots per cell. As evident in Figure 5, rapamycin treatment decreased the amount of virus produced from BCBL-1 cells treated with VPA, TPA, or CoCl2 by 9.3, 9.7, and 7.7 fold, respectively"

Reference: Nichols, L.A., L.A. Adang, and D.H. Kedes, *Rapamycin blocks production of KSHV/HHV8: insights into the anti-tumor activity of an immunosuppressant drug.* PLoS One, 2011. **6**(1): e14535.

~ ~ ~ ~ ~ ~

Modulation of TLR7 signaling in hepatoma cells with HCV infection

Summary: This ImageStream assay measures IRF7 nuclear localization (by quantifying the similarity between the IRF7 and nuclear images on a per-cell basis) in uninfected (Huh) or HCV-replicating (FL, BB7) hepatoma cell lines. The ImageStream's unique ability to objectively measure translocation for thousands of cells per sample allows statistically robust discrimination of the samples, which is of critical importance given their heterogeneous response characteristics. The data show that baseline IRF7 nuclear localization is elevated in HCV-replicating cells (C), yet less sensitive to TLR7 stimulus R837 (D).

"Downstream of TLR7, an increased baseline IRF7 nuclear translocation was observed in HCV-positive cells compared with controls. Stimulation with the TLR7 ligand R837 resulted in significant IRF7 nuclear translocation in control cells. In contrast, HCV-replicating cells showed attenuated TLR7 ligand-induced IRF7 activation. Conclusion: Reduced TLR7 expression, due to RNA instability, directly correlates with HCV replication and alters TLR7-induced IRF7-mediated cell activation. These results suggest a role for TLR7 in HCV-mediated evasion of host immune surveillance."

Reference: Chang, S., K. Kodys, and G. Szabo, *Impaired expression and function of toll-like receptor 7 in hepatitis C virus infection in human hepatoma cells.* Hepatology, 2010. **51**(1): 35-42.

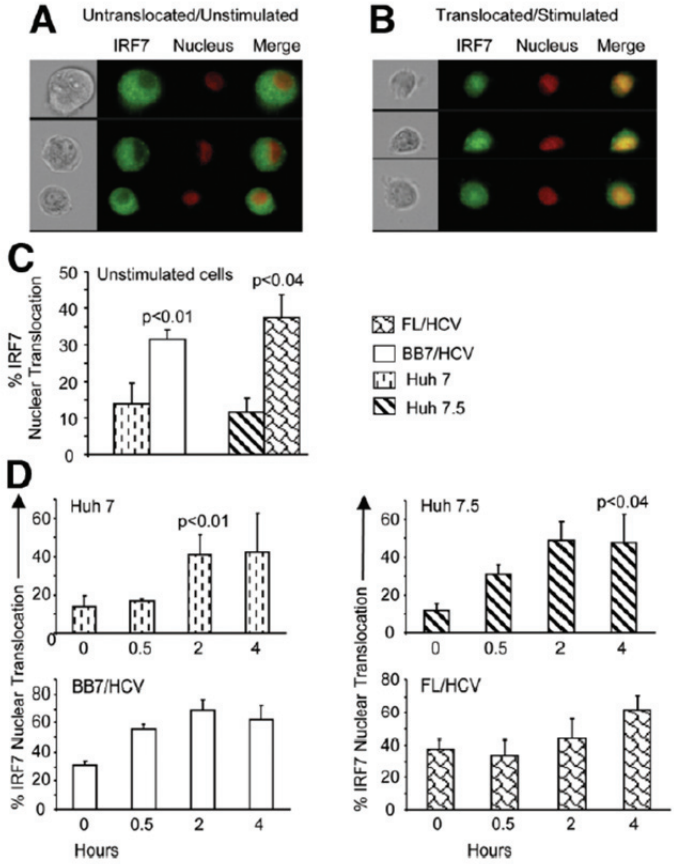

~ ~ ~ ~ ~ ~

uPAR-induced phagocytosis of apoptotic tumor cell fragments

Summary: This ImageStream assay measures the binding and internalization of apoptotic T cell tumor fragments (PKH26) by CS-1 phagocytic cells (GFP+) transfected with Urokinase Plasminogen Activator Receptor (uPAR), β5 integrin, or mock (pCx). Internalization is uniquely measured by quantifying the intensity of the apoptotic material specifically within the internal compartment of the CS-1 cells.

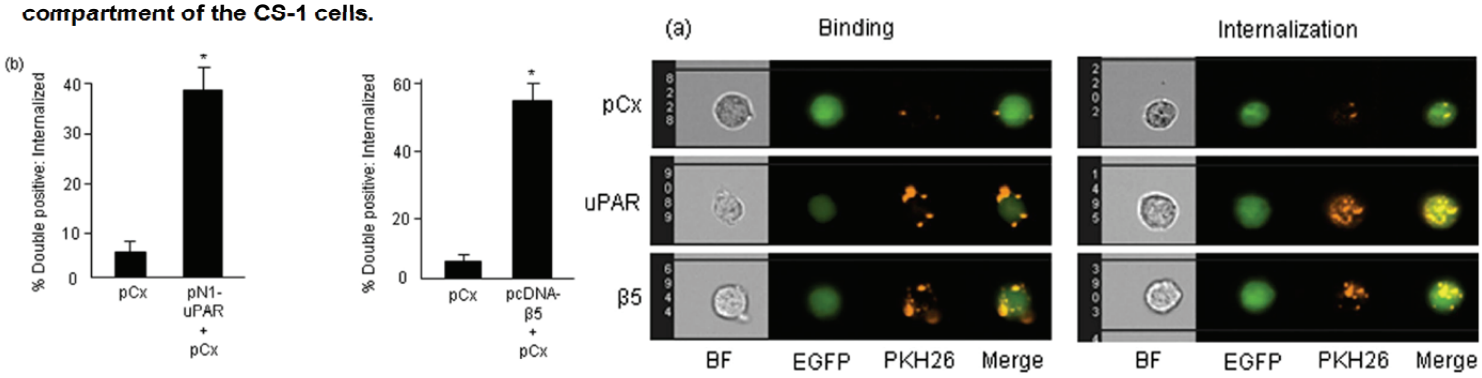

"In the present study, we report that uPAR has a dominant role in the efferocytosis of apoptotic cells, promoting engulfment of apoptotic corpses in transiently overexpressing model phagocytes as well as in breast cancer lines that acquire increased expression of uPAR by epigenetic changes. Because uPAR and the plasminogen activator system are often overexpressed in malignant epithelial carcinomas that include breast, prostate, colon, brain, and others, these data imply that uPAR might confer a phagocytic advantage of uPAR-expressing tumor cells in the tumor microenvironment."

Reference: D'Mello, V., S. Singh, Y. Wu, and R.B. Birge, *The urokinase plasminogen activator receptor promotes efferocytosis of apoptotic cells.* J Biol Chem, 2009. **284**(25): 17030-8.

~ ~ ~ ~ ~ ~

Ofatumamab-mediated complement fixation

Summary: This ImageStream assay measures co-localization of C1q to therapeutic antibody on the surface of B cell tumor cells, indicating that Ofatumamab (OFA) mediates complement fixation. This conclusion is made possible because the ImageStream a) rapidly collects thousands of images per sample for good statistics and b) objective quantifies co-localization on a per-cell basis using the bright detail similarity score.

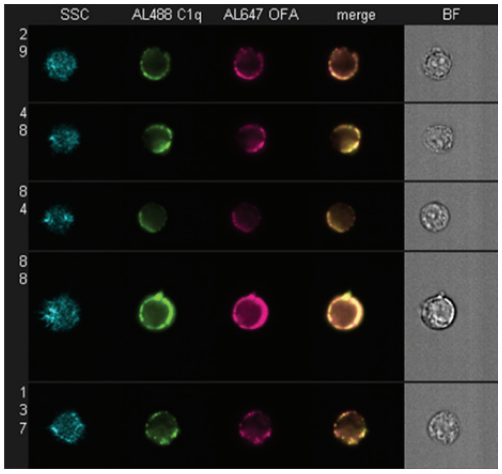

Table I. *Binding of Al488-labeled C1q to mAb-opsonized Daudi cells and colocalization of C1q with mAb*

	Expt. 1			Expt. 2			Expt. 3[a]		
	Al647 mAb (GMF)	Al488 C1q (GMF)	BDSS	Al647 mAb (GMF)	Al488 C1q (GMF)	BDSS	Al647 mAb (GMF)	Al488 C1q (GMF)	BDSS
Al647 OFA	181,000	162,000	3.0	116,000	113,000	3.4	206,000	30,000	2.5
Al647 RTX	186,000	7,500	0.9	61,000	6,600	2.1	155,000	2,200	1.0
Al647 7D8[b]	133,000	2,300	0.6	104,000	1,000	0.9	210,000	1,300	0.7

[a] Different Al488 C1q preparation.
[b] IgG4 (K322A).
BDSS, Bright detail similarity score; GMF, geometric mean fluorescence.

"To test for colocalization quantitatively, double-positive cells (Fig. 2C) were analyzed for colocalization based on an algorithm that calculates the bright detail similarity score. Values of 3–3.5 indicate substantial colocalization, and values of 2.5–3 indicate moderate colocalization. The results of three independent experiments (Table I) reveal that Al488 C1q bound to Al647 OFA-opsonized cells is indeed colocalized with bound OFA."

Reference: Pawluczkowycz, A.W., F.J. Beurskens, P.V. Beum, M.A. Lindorfer, J.G. van de Winkel, P.W. Parren, and R.P. Taylor, *Binding of submaximal C1q promotes complement-dependent cytotoxicity (CDC) of B cells opsonized with anti-CD20 mAbs ofatumumab (OFA) or rituximab (RTX): considerably higher levels of CDC are induced by OFA than by RTX.* J Immunol, 2009. **183**(1): 749-58.

Morphology-based identification of APML

Summary: This ImageStream assay uses the modulation texture feature to objectively discriminate the bright punctate pattern of promyelocytic leukemia protein (PML) associated with normal cells (C and E) from the diffuse pattern associated with APML (D and F). Automated collection of several thousand cells per patient sample enables reporting the percent of cells with aggregated PML as an indicator for APML risk.

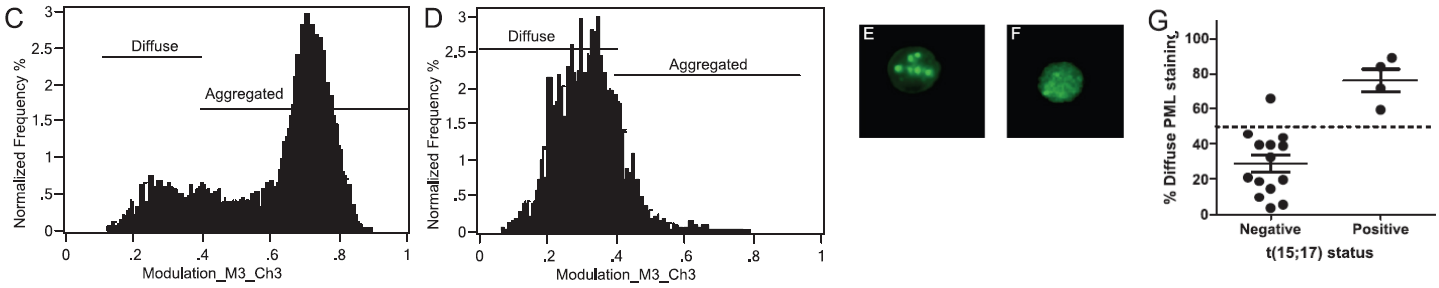

"Acute promyelocytic leukaemia (APML) can be promptly diagnosed by detecting abnormal diffuse staining patterns of PML bodies in abnormal promyelocytes using immunofluorescence microscopy. However, this technique is subjective, with low sensitivity. Using samples from 18 patients with acute myeloid leukaemia (AML) (including four with APML), the authors investigated whether imaging flow cytometry could be a viable alternative to this current technique and improve sensitivity levels. Bone marrow/peripheral blood cells were stained with an antibody to PML, and data were acquired on an ImageStream (Amnis Corporation, Seattle, Washington, USA). Using the modulation feature for data analysis, the authors demonstrated that this technique could successfully identify cases of APML. Imaging flow cytometry, by analysing greater numbers of cells and with the potential to include disease-specific antigens, increases the sensitivity of the current immunofluorescence technique. Imaging flow cytometry is an exciting technology that has many possible applications in the diagnosis of haematological malignancies, including the potential to integrate modalities."

Reference: Grimwade, L., E. Gudgin, D. Bloxham, M.A. Scott, and W.N. Erber, *PML protein analysis using imaging flow cytometry.* J Clin Pathol, 2011. **64**(5): 447-50.

~ ~ ~ ~ ~ ~ ~

CTC detection

Summary: This ImageStream assay combines conventional circulating tumor cell (CTC) immunophenotyping strategies with high resolution imagery for definitive identification of rare tumor cells in whole blood samples. The multiple imaging channels provided by the system afford the opportunity for further functional and phenotypic characterization of CTC.

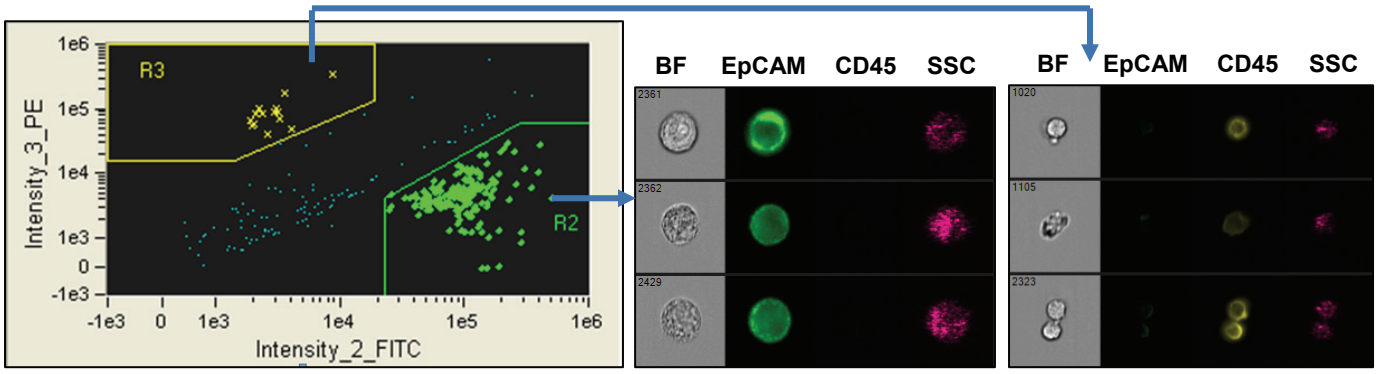

1 mL whole blood spiked with 500 CAMA epithelial tumor cells were enriched using RosetteSep™ CTC Enrichment Cocktail (Stem Cell Tech) and stained with FITC-conjugated anti-epithelial cell antibody (5E11, Stem Cell Tech) and PE-conjugated anti-CD45. The stained samples were then analyzed using an ImageStreamX.

Reference: Presentation at Circulating Tumor Cell Isolation and Diagnostics, 2011, Leiden, NL *Circulating Tumor Cell Detection and Characterization Using the Amnis ImageStreamX System* D Basiji, W Ortyn, CZimmerman, V Venkatachalam, T George, R Kong: http://www.amnis.com/documents/posters/11-001-1-pos%20Lorentz%20CTC.pdf

Aggregation of red blood cells with mononuclear cells in sickle cell disease

Summary: This ImageStream assay measures aggregation between red blood cells (RBC) and mononuclear cells in human sickle cell patient blood samples. RBCs are classically designated as glycophorin A positive and CD45 negative (GPA+ CD45-) whereas RBC-mononuclear cell aggregates are classified as double positive events GPA+ CD45+. Sickle cell patient samples (SS) have an increased level of GPA+ CD45+ events (regions P1-P3) as compared with normal control (AA) as shown in the figure. GPA+ CD45+ events in regions P4 in SS and P5 in AA represent mononuclear cell-RBC derived microparticle aggregates.

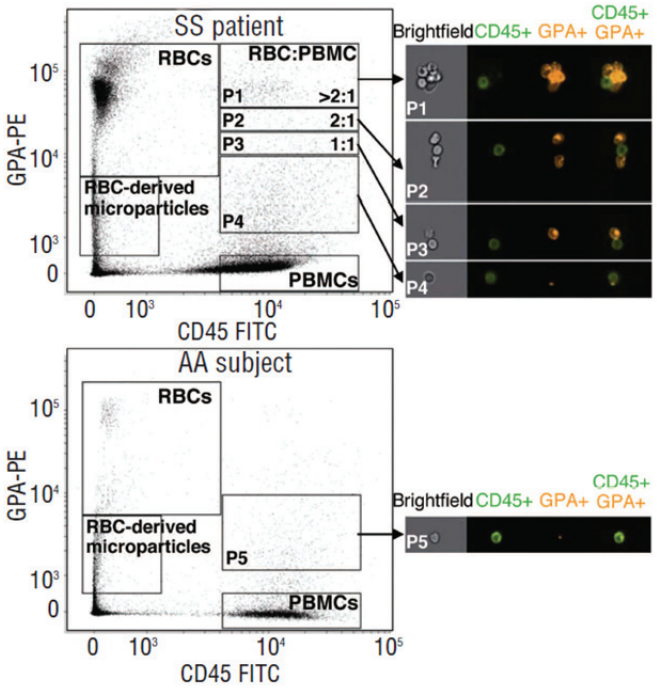

"The imaging flow cytometry revealed that a PBMC could interact with more than one SS RBC in cell aggregates. It also enabled the visualization of aggregates between PBMC and RBC-derived microparticles in both sickle cell disease patients and AA controls. The imaging flow cytometry assay was essential to determine the composition of the aggregates and to optimize the gating in the classical flow cytometry assays that followed, taking into account aggregates comprising whole cells and excluding those with RBC-derived microparticles."

Reference: Chaar, V., J. Picot, O. Renaud, P. Bartolucci, R. Nzouakou, D. Bachir, F. Galacteros, Y. Colin*, et al.*, *Aggregation of mononuclear and red blood cells through an {alpha}4{beta}1-Lu/basal cell adhesion molecule interaction in sickle cell disease.* Haematologica, 2010. **95**(11): 1841-8.

~ ~ ~ ~ ~ ~

Mobilization of Oct-4 pluripotent stem cells in ischemic heart disease

Summary: This ImageStream assay quantifies the number of circulating Lin$^-$/CD45$^-$/CD34$^+$/Oct4$^+$ stem cells in patients with ischemic heart disease and normal patient controls. Peripheral blood samples from normal and ischemic patients were analyzed for the presence of Oct4$^+$ pluripotent VSELs as shown in (A) and (B) compared with SSEA4$^+$ cells in (C).

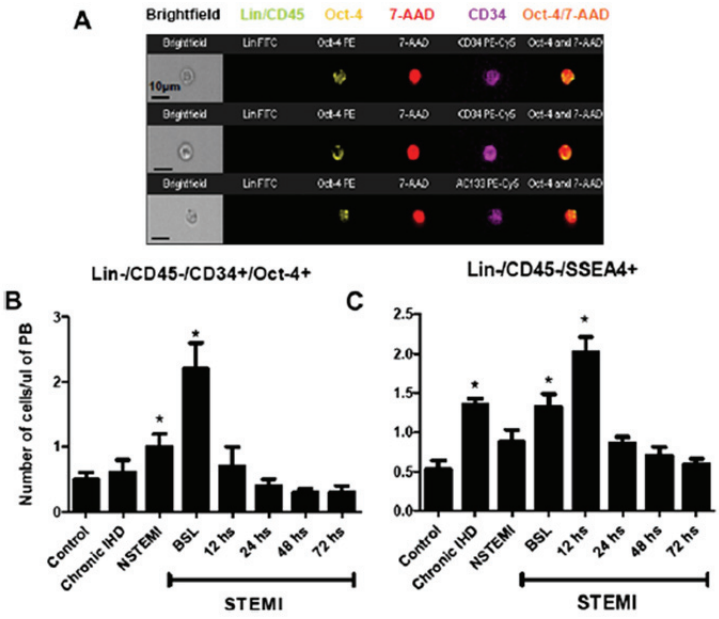

"Based on the unique capabilities of ISS technology, we were able to quantify PSCs accurately by distinguishing real intranuclear Oct-4 expression from false positives events."

Reference: Abdel-Latif, A., E.K. Zuba-Surma, K.M. Ziada, M. Kucia, D.A. Cohen, A.M. Kaplan, G. Van Zant, S. Selim*, et al.*, *Evidence of mobilization of pluripotent stem cells into peripheral blood of patients with myocardial ischemia.* Exp Hematol, 2010. **38**(12): 1131-1142 e1.

Morphological classification of erythroid progenitor populations

Summary: This ImageStream assay distinguishes erythroid progenitor populations in murine bone marrow using image analysis of both intensity as well as morphology parameters. The mean pixel intensities (total intensity divided by area of the intensity) of Ter119 and DRAQ5 are used in combination with nuclear size (area) to classify erythroid populations as shown in the gating strategy in (A-F). Representative images of each population are shown in (G).

"The multispectral imaging of cells in flow, in adherent cultures or in tissues will be an important new tool that can be used with standard flow cytometry as well as histologic microscopy. The power to analyze the images of large numbers of cells will greatly improve our ability to detect complex and relatively rare populations compared to standard histological approaches. Quantitation of sub-cellular and complex morphologic features alongside multiple measurements of fluorescence intensity will also greatly improve our understanding of the cells analyzed by flow cytometry."

Reference: McGrath, K.E., T.P. Bushnell, and J. Palis, Multispectral imaging of hematopoietic cells: where flow meets morphology. J Immunol Methods, 2008. 336(2): 91-7.

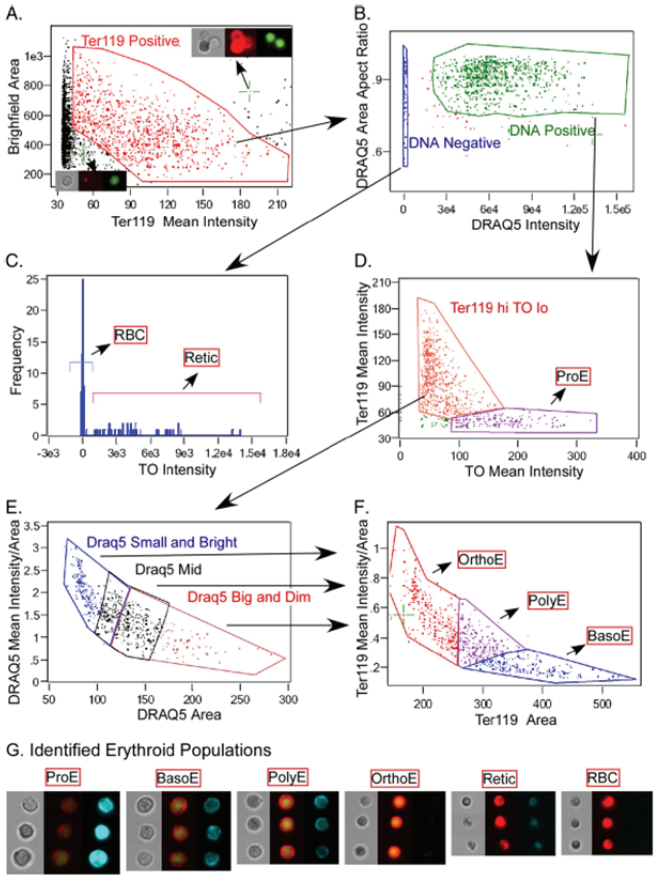

~ ~ ~ ~ ~ ~

Measurment of adipogenic activity in primary human fibroblasts

Summary: This ImageStream assay measures adipogenic activity in primary human fibroblasts by fluorescence quantification of the neutral lipid dye LipidTox (LTX). Adipocytes are identified as those events with high LTX intensity and high LTX texture (using Frequency parameter, which measures the standard deviation of the pixels in the LTX image).

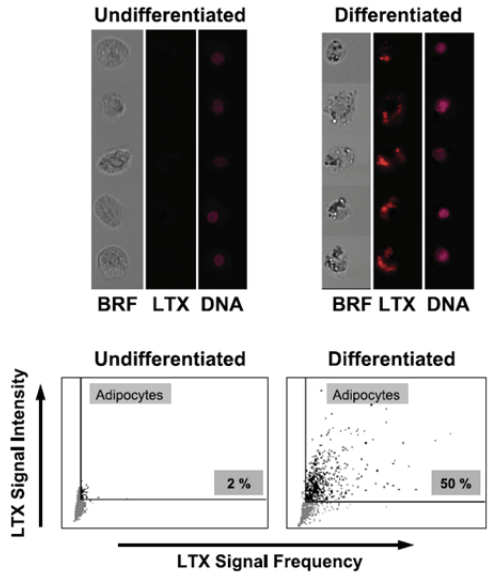

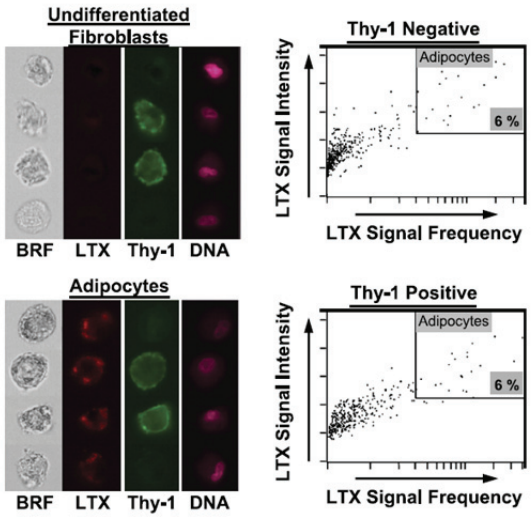

"This technology makes it possible both to observe the accumulation of intracellular lipid on a per cell basis and to quantitate adipocyte frequency over a large number of cells. It also facilitates the simultaneous observation of Thy-1 expression with lipid accumulation.

Using this technique, we were surprised to learn that Thy-1-positive cells are not precluded from differentiating into adipocytes. In a mixed culture, the frequency of Thy-1-positive adipocytes is approximately equal to that of Thy-1 negative adipocytes. However, imaging flow cytometry confirms that purified populations of Thy-1-positive fibroblasts do not differentiate in response to 15d-PGJ2, whereas purified Thy-1-negative populations do differentiate."

Reference: Lehmann, G.M., C.F. Woeller, S.J. Pollock, C.W. O'Loughlin, S. Gupta, S.E. Feldon, and R.P. Phipps, *Novel anti-adipogenic activity produced by human fibroblasts.* Am J Physiol Cell Physiol, 2010. **299**(3): C672-81.

~ ~ ~ ~ ~ ~

Measurement of monocyte shape change in response to chemokine stimulation

Summary: This ImageStream assay quantifies cell shape change after chemokine treatment. Human whole blood was treated with the chemokine MCP-1, fixed and labeled with CD14 antibody and large event files were collected. Cell shape was quantified using the circularity feature, which the IDEAS software ranked as the best discriminating parameter (amongst 70 candidate shape-based parameters, histogram; table shows the top 10 parameters) for the hand-picked round and elongated cells in (A). Circularity scores for CD14+ cells from untreated (left) and MCP-1 treated (right) blood are shown in (B).

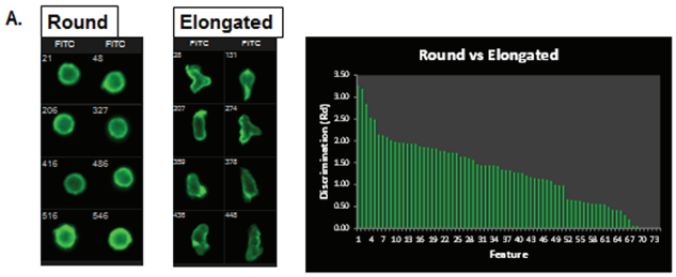

	Discrimination Power	
Feature	Rank	Rd
Circularity_M03	1	3.27
Circularity_Object(M8, FITC, Tight)	2	3.18
Circularity_Morphology(M3, FITC)	3	2.84
Shape Ratio_Object(M3, FITC, Tight)	4	2.52
Shape Ratio_M3	5	2.49
Aspect Ratio_Morphology(M3, FITC)	6	2.14
Aspect Ratio_Object(M3, Tight)	7	2.13
Aspect Ratio_M3	8	2.08
MajorAxis_Morphology(M3, FITC)	9	2.01
Symmetry 2_M3_FITC	10	1.97

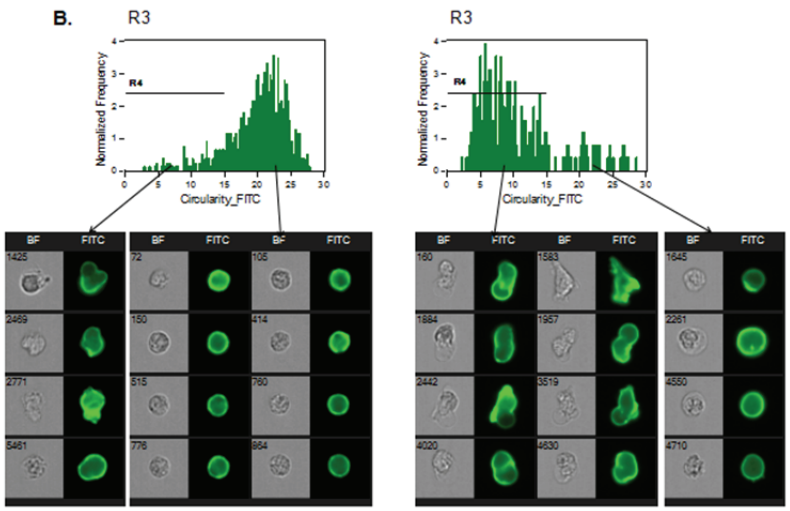

"Migration is traditionally measured in vitro using transwell assays, which can be a labor-intensive and time-consuming assay. Here we describe a simple method using ImageStream cytometry for measuring monocyte shape change directly in whole blood samples exposed to chemoattractant."

Reference: T.C. George, B.E. Hall, S.M. Mordecai, S.L. Friend, R. Kong, and R DeMarco. *Analysis of whole blood immune function using imaging flow cytometry.* Poster presentation AAI 2011.

Reference list – Clinical research applications for the ImageStream

Abdel-Latif, A., E.K. Zuba-Surma, K.M. Ziada, M. Kucia, D.A. Cohen, A.M. Kaplan, G. Van Zant, S. Selim*, et al.*, *Evidence of mobilization of pluripotent stem cells into peripheral blood of patients with myocardial ischemia.* Exp Hematol, 2010. **38**(12): 1131-1142 e1.

Ackerman, M.E., B. Moldt, R.T. Wyatt, A.S. Dugast, E. McAndrew, S. Tsoukas, S. Jost, C.T. Berger*, et al.*, *A robust, high-throughput assay to determine the phagocytic activity of clinical antibody samples.* J Immunol Methods, 2011. **366**(1-2): 8-19.

Adang, L.A., C.H. Parsons, and D.H. Kedes, *Asynchronous progression through the lytic cascade and variations in intracellular viral loads revealed by high-throughput single-cell analysis of Kaposi's sarcoma-associated herpesvirus infection.* J Virol, 2006. **80**(20): 10073-82.

Beum, P.V., M.A. Lindorfer, B.E. Hall, T.C. George, K. Frost, P.J. Morrissey, and R.P. Taylor, *Quantitative analysis of protein co-localization on B cells opsonized with rituximab and complement using the ImageStream multispectral imaging flow cytometer.* J Immunol Methods, 2006. **317**(1-2): 90-9.

Beum, P.V., D.A. Mack, A.W. Pawluczkowycz, M.A. Lindorfer, and R.P. Taylor, *Binding of rituximab, trastuzumab, cetuximab, or mAb T101 to cancer cells promotes trogocytosis mediated by THP-1 cells and monocytes.* J Immunol, 2008. **181**(11): 8120-32.

Chaar, V., J. Picot, O. Renaud, P. Bartolucci, R. Nzouakou, D. Bachir, F. Galacteros, Y. Colin*, et al.*, *Aggregation of mononuclear and red blood cells through an {alpha}4{beta}1-Lu/basal cell adhesion molecule interaction in sickle cell disease.* Haematologica, 2010. **95**(11): 1841-8.

Chang, S., K. Kodys, and G. Szabo, *Impaired expression and function of toll-like receptor 7 in hepatitis C virus infection in human hepatoma cells.* Hepatology, 2010. **51**(1): 35-42.

D'Mello, V., S. Singh, Y. Wu, and R.B. Birge, *The urokinase plasminogen activator receptor promotes efferocytosis of apoptotic cells.* J Biol Chem, 2009. **284**(25): 17030-8.

Elliott, G.S., *Moving Pictures: Imaging Flow Cytometry for Drug Development.* Combinatorial Chemistry & High Throuput Screening, 2009. **12**: 849-859.

Field, J.J., D.G. Nathan, and J. Linden, *Targeting iNKT cells for the treatment of sickle cell disease.* Clin Immunol, 2011.

Gandillet, A., S. Park, F. Lassailly, E. Griessinger, J. Vargaftig, A. Filby, T.A. Lister, and D. Bonnet, *Heterogeneous sensitivity of human acute myeloid leukemia to beta-catenin down-modulation.* Leukemia, 2011. **25**(5): 770-80.

Grimwade, L., E. Gudgin, D. Bloxham, M.A. Scott, and W.N. Erber, *PML protein analysis using imaging flow cytometry.* J Clin Pathol, 2011. **64**(5): 447-50.

Hassman, L.M., T.J. Ellison, and D.H. Kedes, *KSHV infects a subset of human tonsillar B cells, driving proliferation and plasmablast differentiation.* J Clin Invest, 2011. **121**(2): 752-68.

Helguera, G., J.A. Rodriguez, R. Luria-Perez, S. Henery, P. Catterton, C. Bregni, T.C. George, O. Martinez-Maza*, et al.*, *Visualization and quantification of cytotoxicity mediated by antibodies using imaging flow cytometry.* J Immunol Methods, 2011. **368**(1-2): 54-63.

Lehmann, G.M., C.F. Woeller, S.J. Pollock, C.W. O'Loughlin, S. Gupta, S.E. Feldon, and R.P. Phipps, *Novel anti-adipogenic activity produced by human fibroblasts.* Am J Physiol Cell Physiol, 2010. **299**(3): C672-81.

Lepelley, A., S. Louis, M. Sourisseau, H.K. Law, J. Pothlichet, C. Schilte, L. Chaperot, J. Plumas*, et al.*, *Innate Sensing of HIV-Infected Cells.* PLoS Pathog, 2011. **7**(2): e1001284.

Maguire, O., C. Collins, K. O'Loughlin, J. Miecznikowski, and H. Minderman, *Quantifying nuclear p65 as a parameter for NF-kappaB activation: Correlation between ImageStream cytometry, microscopy, and Western blot.* Cytometry A, 2011. **79**(6): 461-9.

McGrath, K.E., T.P. Bushnell, and J. Palis, *Multispectral imaging of hematopoietic cells: where flow meets morphology.* J Immunol Methods, 2008. **336**(2): 91-7.

McGrath, K.E., J.M. Frame, G.J. Fromm, A.D. Koniski, P.D. Kingsley, J. Little, M. Bulger, and J. Palis, *A transient definitive erythroid lineage with unique regulation of the {beta}-globin locus in the mammalian embryo.* Blood, 2011. **117**(17): 4600-8.

Megjugorac, N.J., E.S. Jacobs, A.G. Izaguirre, T.C. George, G. Gupta, and P. Fitzgerald-Bocarsly, *Image-based study of interferongenic interactions between plasmacytoid dendritic cells and HSV-infected monocyte-derived dendritic cells.* Immunol Invest, 2007. **36**(5-6): 739-61.

Nichols, L.A., L.A. Adang, and D.H. Kedes, *Rapamycin blocks production of KSHV/HHV8: insights into the anti-tumor activity of an immunosuppressant drug.* PLoS One, 2011. **6**(1): e14535.

Nobile, C., D. Rudnicka, M. Hasan, N. Aulner, F. Porrot, C. Machu, O. Renaud, M.C. Prevost*, et al.*, *HIV-1 Nef inhibits ruffles, induces filopodia, and modulates migration of infected lymphocytes.* J Virol, 2010. **84**(5): 2282-93.

Pawluczkowycz, A.W., F.J. Beurskens, P.V. Beum, M.A. Lindorfer, J.G. van de Winkel, P.W. Parren, and R.P. Taylor, *Binding of submaximal C1q promotes complement-dependent cytotoxicity (CDC) of B cells opsonized with anti-CD20 mAbs ofatumumab (OFA) or rituximab (RTX): considerably higher levels of CDC are induced by OFA than by RTX.* J Immunol, 2009. **183**(1): 749-58.

Petrovas, C., B. Chaon, D.R. Ambrozak, D.A. Price, J.J. Melenhorst, B.J. Hill, C. Geldmacher, J.P. Casazza*, et al.*, *Differential association of programmed death-1 and CD57 with ex vivo survival of CD8+ T cells in HIV infection.* J Immunol, 2009. **183**(2): 1120-32.

Pietzsch, J., J.F. Scheid, H. Mouquet, F. Klein, M.S. Seaman, M. Jankovic, D. Corti, A. Lanzavecchia*, et al.*, *Human anti-HIV-neutralizing antibodies frequently target a conserved epitope essential for viral fitness.* J Exp Med, 2010. **207**(9): 1995-2002.

Ploppa, A., T.C. George, K.E. Unertl, B. Nohe, and M.E. Durieux, *ImageStream cytometry extends the analysis of phagocytosis and oxidative burst.* Scand J Clin Lab Invest, 2011.

Riddell, J.R., X.Y. Wang, H. Minderman, and S.O. Gollnick, *Peroxiredoxin 1 stimulates secretion of proinflammatory cytokines by binding to TLR4.* J Immunol, 2010. **184**(2): 1022-30.

Santer, D.M., B.E. Hall, T.C. George, S. Tangsombatvisit, C.L. Liu, P.D. Arkwright, and K.B. Elkon, *C1q deficiency leads to the defective suppression of IFN-alpha in response to nucleoprotein containing immune complexes.* J Immunol, 2010. **185**(8): 4738-49.

Sharma, P.K., R. Singh, K.R. Novakovic, J.W. Eaton, W.E. Grizzle, and S. Singh, *CCR9 mediates PI3K/AKT-dependent antiapoptotic signals in prostate cancer cells and inhibition of CCR9-CCL25 interaction enhances the cytotoxic effects of etoposide.* Int J Cancer, 2010. **127**(9): 2020-30.

Singh, S., R. Singh, U.P. Singh, S.N. Rai, K.R. Novakovic, L.W. Chung, P.J. Didier, W.E. Grizzle*, et al.*, *Clinical and biological significance of CXCR5 expressed by prostate cancer specimens and cell lines.* Int J Cancer, 2009. **125**(10): 2288-95.

Xu, C., A. Lo, A. Yammanuru, A.S. Tallarico, K. Brady, A. Murakami, N. Barteneva, Q. Zhu*, et al.*, *Unique biological properties of catalytic domain directed human anti-CAIX antibodies discovered through phage-display technology.* PLoS One, 2010. **5**(3): e9625.

Yan, Y., A.P. Johnston, S.J. Dodds, M.M. Kamphuis, C. Ferguson, R.G. Parton, E.C. Nice, J.K. Heath*, et al.*, *Uptake and intracellular fate of disulfide-bonded polymer hydrogel capsules for Doxorubicin delivery to colorectal cancer cells.* ACS Nano, 2010. **4**(5): 2928-36.